Electronic Supplementary Material (ESI) for ChemComm.


# Supporting information

## One step synthesis of boron-doped carbon nitride derived from 4-pyridylboronic acid as biosensing platforms for assessment of food safety

Xiaxia Li,[a] Peiyao Zhu,[a] Chunsen Liu,[b] Huan Pang,*[a]

[a]School of Chemistry and Chemical Engineering, Institute for Innovative Materials and Energy, Yangzhou University, Yangzhou, 225009, Jiangsu, P. R. China.

[b]Henan Provincial Key Lab of Surface & Interface Science, Zhengzhou University of Light Industry, Zhengzhou, Henan 450002, China

**Table of Contents**

**Experimental Section**

The BCN nanonanosheets were synthesized by heating the 4-pyridylboronic acid in a pipe furnace. A certain amount 4-pyridylboronic acid with corundum boat was placed in pipe furnace. The pipe furnace is heated to 700, 800, and 900 $^{o}$C in $N_2$ atmosphere, donated as BCN-700, BCN-800, and BCN-900, respectively. After the samples cooled to room temperature. The synthesized samples are collected.

**Fabrication of the electrochemical immunosensors based on BCN materials**

To develop the immunosensors, BCN were dispersed into fresh Milli-Q water at concentration of 1.0 mg $mL^{-1}$. The prepared solutions (10.0 μL) were dropped into clean gold electrodes. Finally, the modified electrodes were dried in $N_2$ stream for further testing. The modified AEs were incubated separately with the solutions of $Anti_{vomitoxin}$ and $Anti_{salbutamol}$ (10 ng $mL^{-1}$) for 2 h (Anti/BCN/AE) at room temperature. Subsequently, the modified AEs adsorbed with antibodies were sufficiently rinsed with PBS and then dried over a gentle stream of nitrogen, through which the developed immunosensors were accomplished. Further measurements were performed. When not in use, the immunosensors were stored at 4 °C in a refrigerator.

**Characterization**

The products were tested by X-ray diffraction (XRD) on a Bruker D8 Advanced X-ray Diffractometer (Cu-Kα radiation: λ=0.15406 nm) for the phase analysis. Scanning electron microscope (SEM, Zeiss_Supra55) was used for observing the morphology of the samples at an acceleration voltage of 5.0 kV. High-resolution transmission electron microscopy (HRTEM) images, selected area electron diffraction (SAED) images, and energy dispersive X-ray spectroscopy mapping were captured on a Tecnai G2 F30 transmission electron microscopy at an acceleration voltage of 300 kV. X-ray photoelectron spectroscopy (XPS) was carried out on a Thermo Scientific ESCALAB 250 apparatus.

**Electrochemical Measurements**

All electrochemical measurements, including electrochemical impedance spectroscopy (EIS) and cyclic voltammetry (CV), were conducted on a CHI760E electrochemical workstation (Shanghai Chenhua, China). A conventional three-electrode system, which included a gold electrode with a diameter of 3 mm as a working electrode, an Ag/AgCl (saturated KCl) electrode as a reference electrode, and a platinum slide as a counter electrode, was used. EIS curves were obtained in 0.5 mM $[Fe(CN)_6]^{3-/4-}$ containing 0.1 M KCl (EIS parameters: potential, 0.21 V; frequency range, 100-0.1 Hz; amplitude, 5 mV; room temperature). incubation and test temperature are room-temperature. The EIS spectra were analyzed using Zview2 software, which utilizes nonlinear least-squares fitting to determine element parameters in the equivalent circuit.

**Materials and reagents**

All chemicals, 4-pyridylboronic acid was purchased from Shanghai Sinopharm Chemical Reagent and used without further treatment or purification. Oxytetracycline (TET), doxycycline (DOX), kanamycin, ofloxacin, streptomycin (1.0 ng $mL^{-1}$), vomitoxin, salbutamol, the antibody of vomitoxin and salbutamol ($Anti_{vomitoxin}$, $Anti_{salbutamol}$), were obtained from

Solarbio Life Sciences Co., Ltd. Both $[Fe(CN)_6]^{3-/4-}$ and phosphate-buffered solution (PBS) (pH 7.4, NaCl; $Na_2HPO_3$; $KH_2PO_4$; KCl) were obtained from Aladdin Co., Ltd. All other chemicals used in this study were analytical grade reagents.

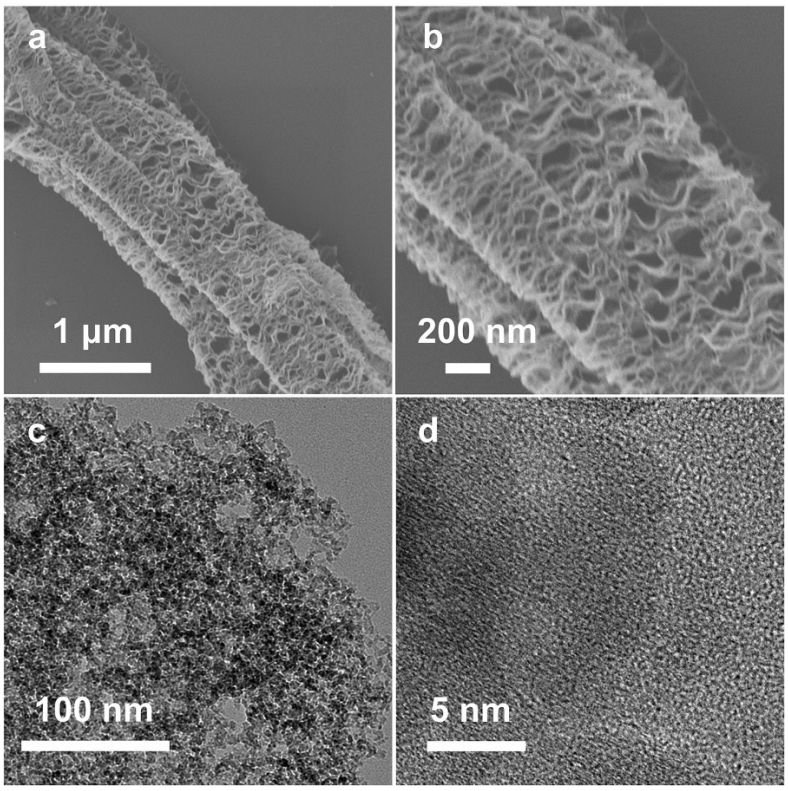


**Figure S1.** (a, b) SEM images of BCN-700. (c, d) HRTEM images of BCN-700.

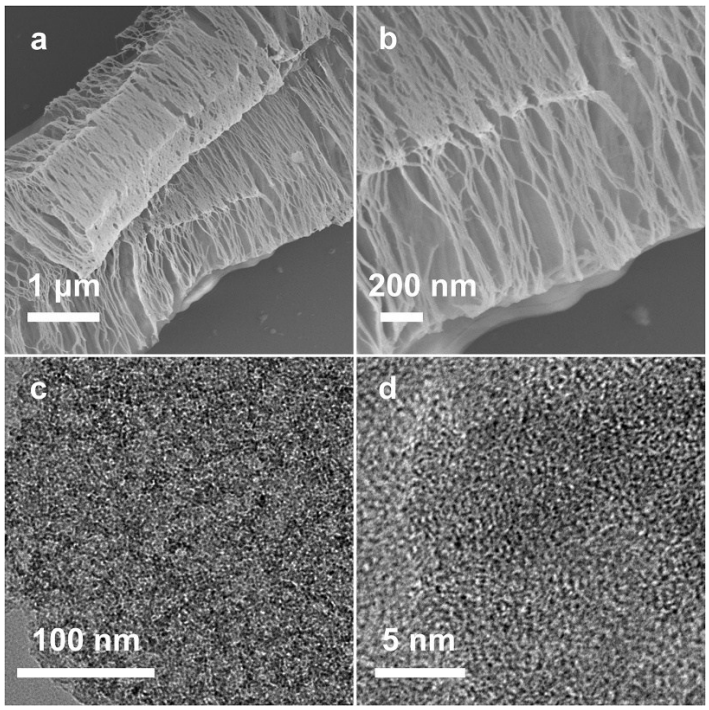


**Figure S2.** (a, b) SEM images of BCN-900. (c, d) HRTEM images of BCN-900.

The progress of 4-pyridylboronic acid calcined to prepare BCN nanosheets was followed by thermo-gravimetric analysis (TGA) curve as shown in **Figure S3**. The first mass loss stage (ca. 14.1%) from 100 $^{o}$C to 190 $^{o}$C. The drastic mass loss (ca. 33.4%) from 450 $^{o}$C to 500 $^{o}$C, slow mass loss (ca. 2%) from 200 $^{o}$C to 380 $^{o}$C. Another mass loss (ca. 20%) from 380 $^{o}$C to 900 $^{o}$C were observed.

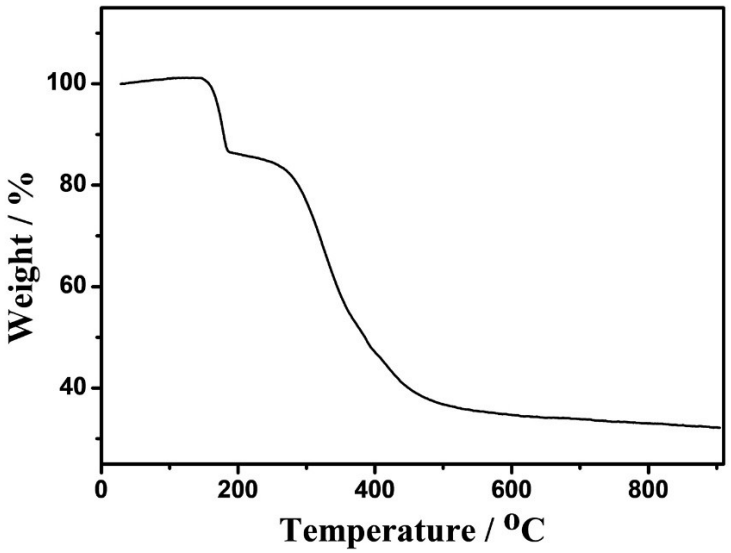


**Figure S3.** TGA of 4-pyridylboronic acid.

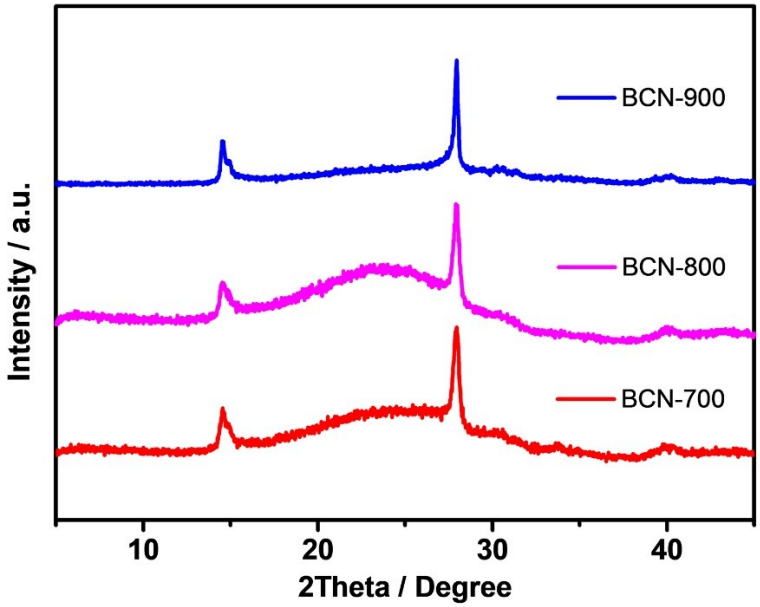


**Figure S4.** XRD patterns of the BCN-700, BCN-800, and BCN-900.

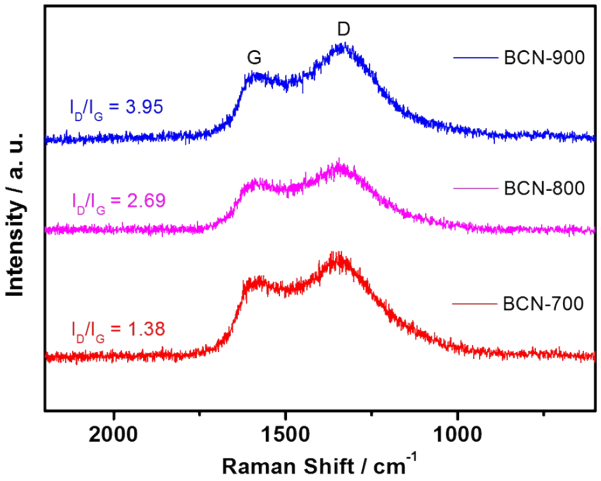


**Figure S5.** Raman spectra of the BCN-700, BCN-800, and BCN-900.

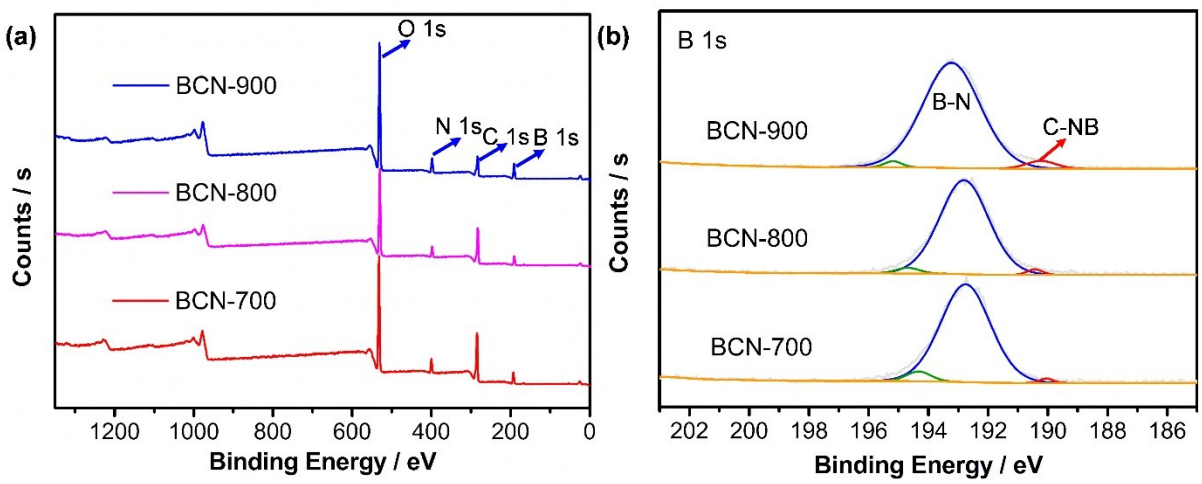


**Figure S6** (a) The survey spectrum and (b) B 1s spectrum of the BCN-700, BCN-800, and BCN-900.

The EIS spectra were analyzed using Zview2 software. A nonlinear least-squares method was used to fit and determine the parameters of the elements in an equivalent circuit (Figure S6). The Randles equivalent circuit, which consists of solution resistance ($R_s$), charge-transfer resistance ($R_{ct}$), constant-phase element (CPE), and Warburg impedance ($W_o$), was shown in the inset of Figure S6.

As shown in the typical EIS spectrum (Figure S6), the Z' (real part) versus Z'' (imaginary part) means that the electron-transfer resistance ($R_{ct}$) at the electrode surface was the same as the diameter of the semicircle on the Nyquist plot and can be used to describe the properties at the interface between the electrode and analyte solution.[1-3] The Nyquist plot is composed of two sections: the semicircle part at higher frequencies belonging to the electron-transfer limited process and the linear portion at lower frequency range corresponding to the diffusion-limited process.

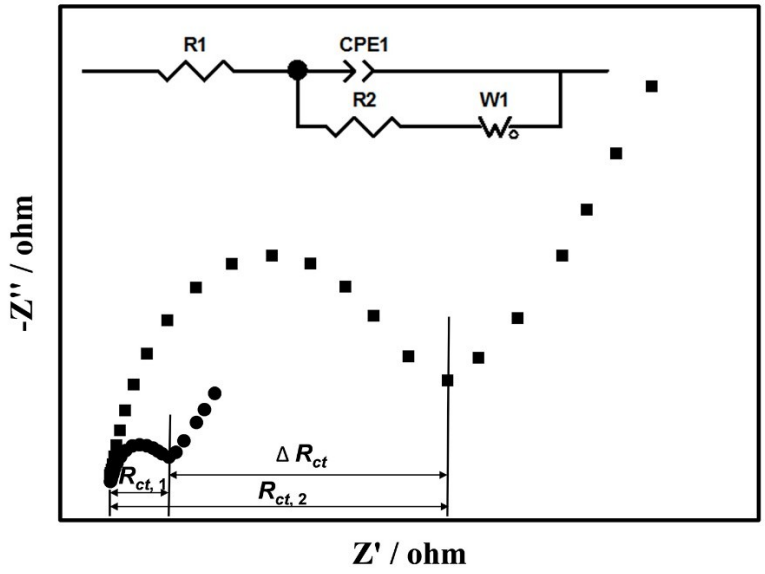


**Figure S7.** The typical EIS Nyquist plot and equivalent circuit.

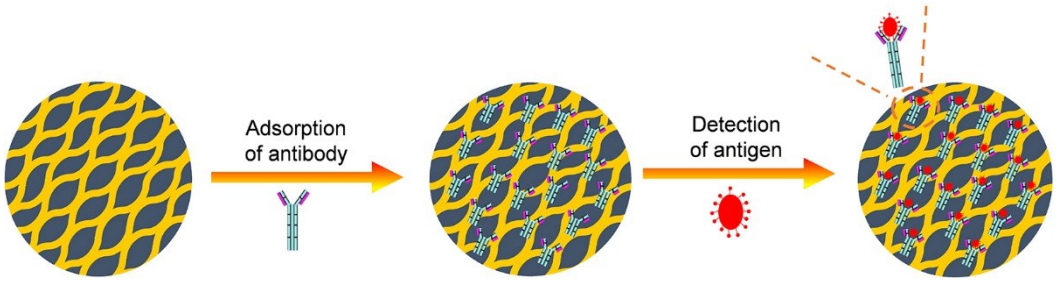


**Scheme S1** The BCN nanosheet adsorption of antibody and detection of antigen.

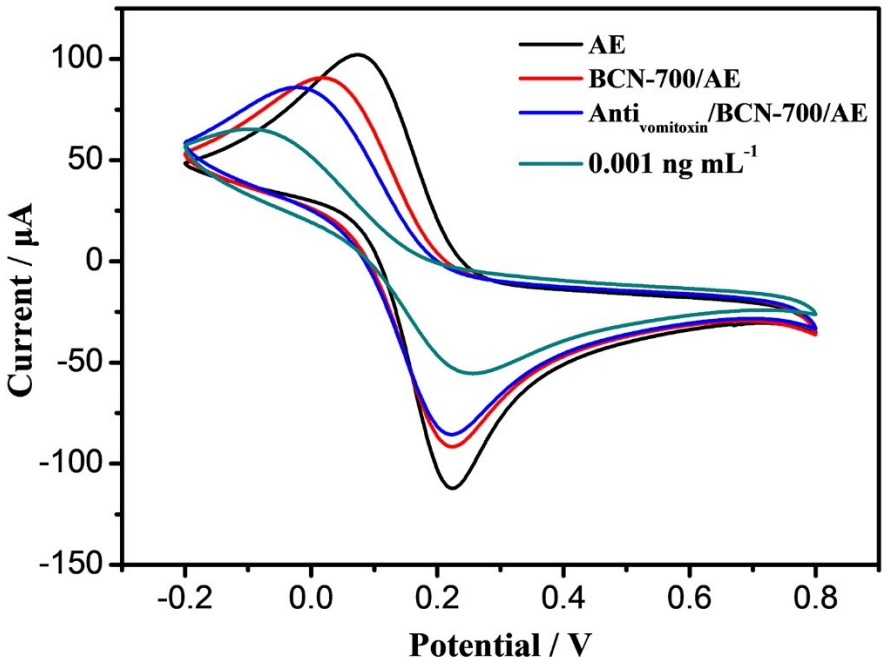


**Figure S8.** CV at a scan rate of 100 mV $s^{-1}$ of vomitoxin detection using the developed biosensor based on BCN-700 in 5 mM $[Fe(CN)_6]^{3-/4-}$ containing 0.14 M NaCl and 0.1 M KCl: AE, BCN-700/AE, $Anti_{vomitoxin}$/BCN-700/AE, 0.001 ng $mL^{-1}$ vomitoxin.

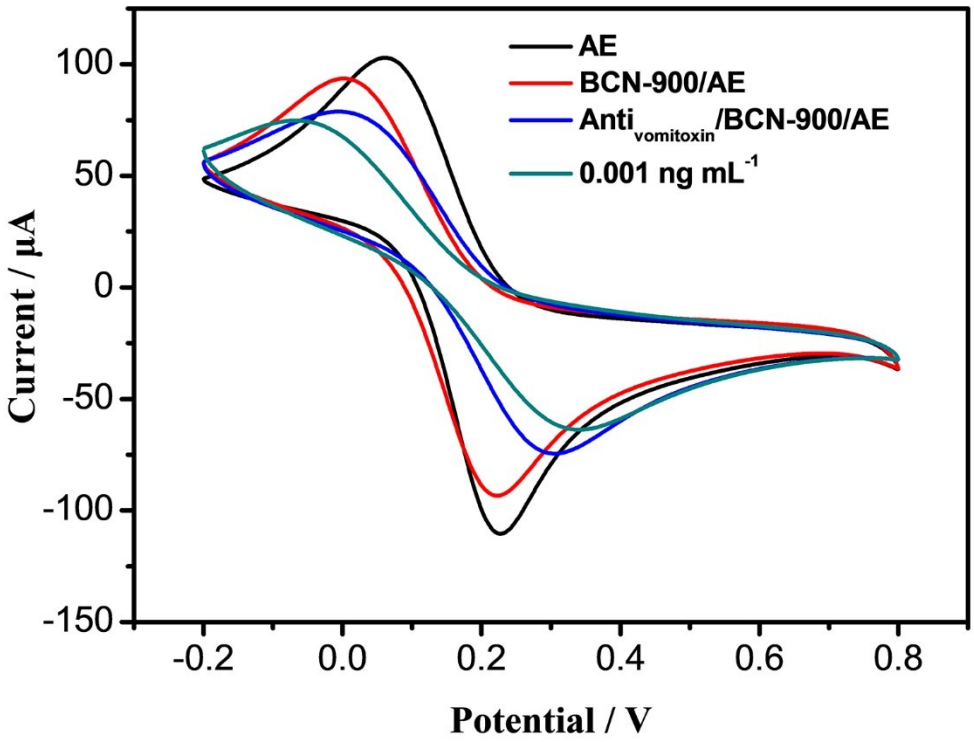


**Figure S9.** CV at a scan rate of 100 mV $s^{-1}$ of vomitoxin detection using the developed biosensor based on BCN-900 in 5 mM $[Fe(CN)_6]^{3-/4-}$ containing 0.14 M NaCl and 0.1 M KCl: AE, BCN-900/AE, $Anti_{vomitoxin}$/BCN-900/AE, 0.001 ng $mL^{-1}$ vomitoxin.

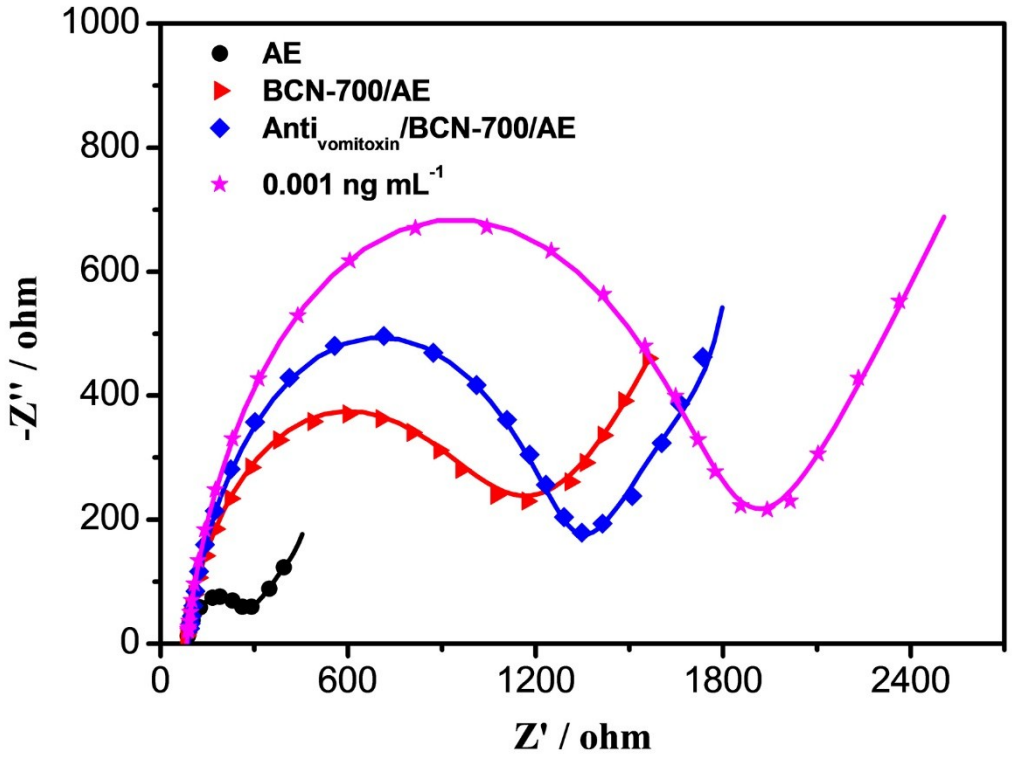


**Figure S10.** EIS plots tracing the whole procedure of vomitoxin detection using the developed biosensor based on BCN-700 in 5 mM $[Fe(CN)_6]^{3-/4-}$ containing 0.14 M NaCl and 0.1 M KCl: AE, BCN-700/AE, $Anti_{vomitoxin}$/BCN-700/AE, 0.001 ng $mL^{-1}$ vomitoxin.

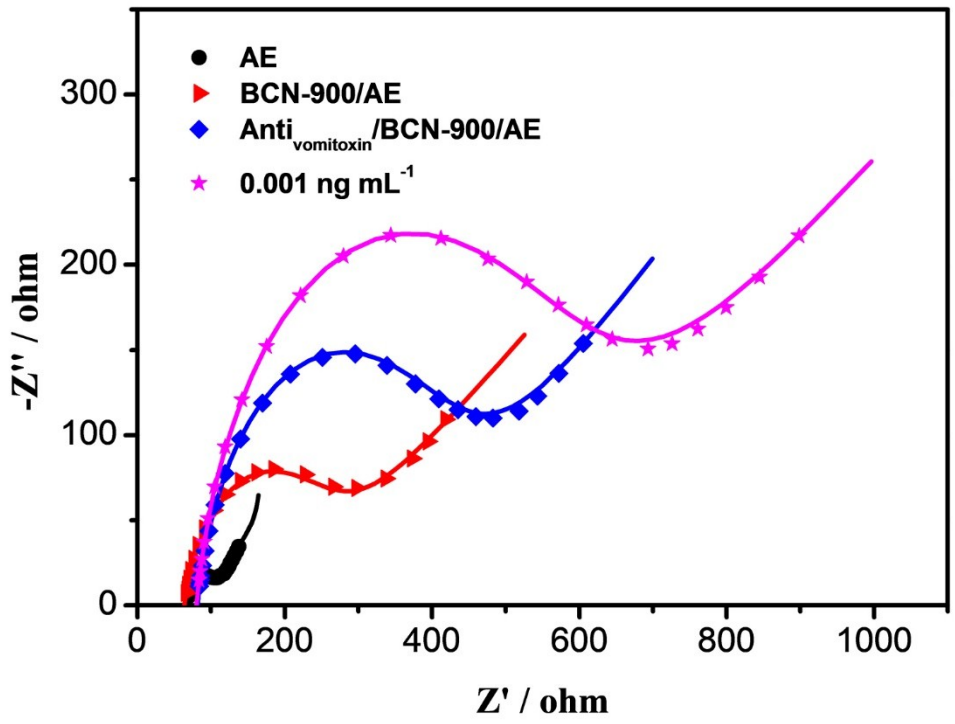


**Figure S11.** EIS plots tracing the whole procedure of vomitoxin detection using the developed biosensor based on BCN-900 in 5 mM $[Fe(CN)_6]^{3-/4-}$ containing 0.14 M NaCl and 0.1 M KCl: AE, BCN-900/AE, $Anti_{vomitoxin}$/BCN-900/AE, 0.001 ng $mL^{-1}$ vomitoxin.

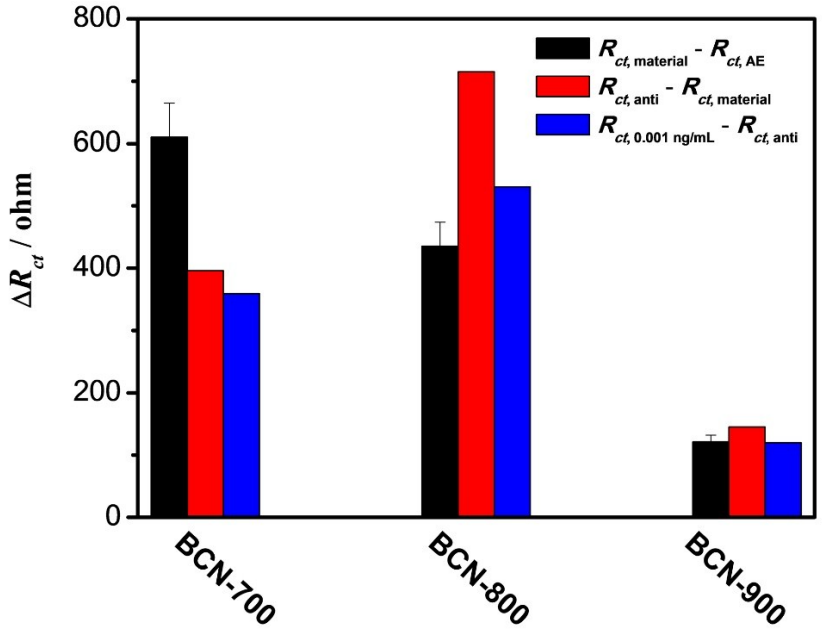


**Figure S12.** Differences in $\Delta R_{ct}$ values at each stage for the vomitoxin detection using the developed immunosensors based on BCN-700, BCN-800, and BCN-900.

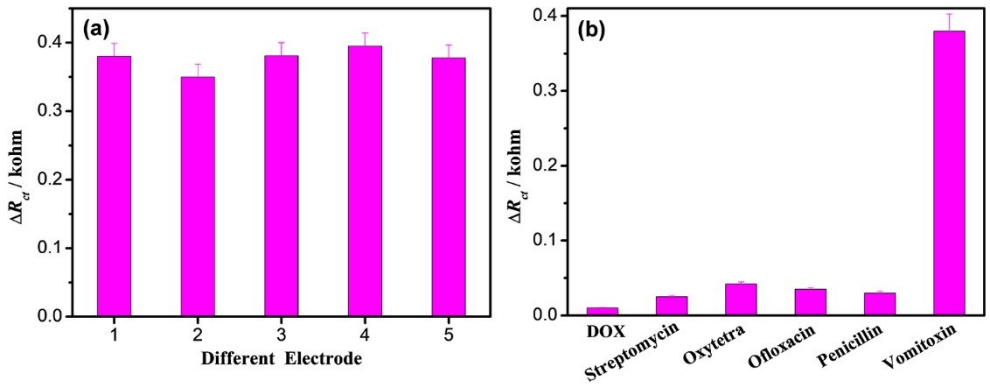


**Figure S13.** (a) Reproducibility and (b) selectivity studies of the BCN-800 electrochemical immunosensor toward vomitoxin. EIS experiments were performed with 1 ng $mL^{-1}$ each of DOX, streptomycin, oxytetra, ofloxacin, and penicillin, as well as 0.001 ng $mL^{-1}$ vomitoxin.

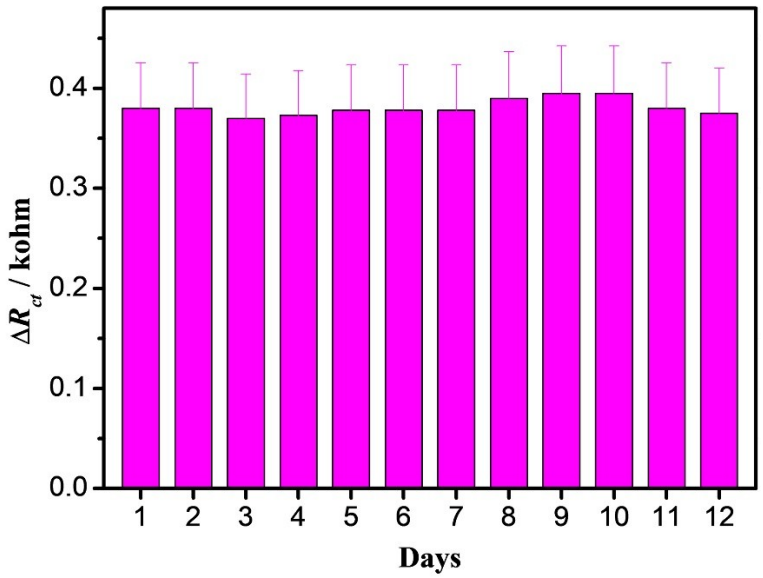


**Figure S14.** Stability of the BCN-800 electrochemical immunosensor toward detecting vomitoxin within 12 days.

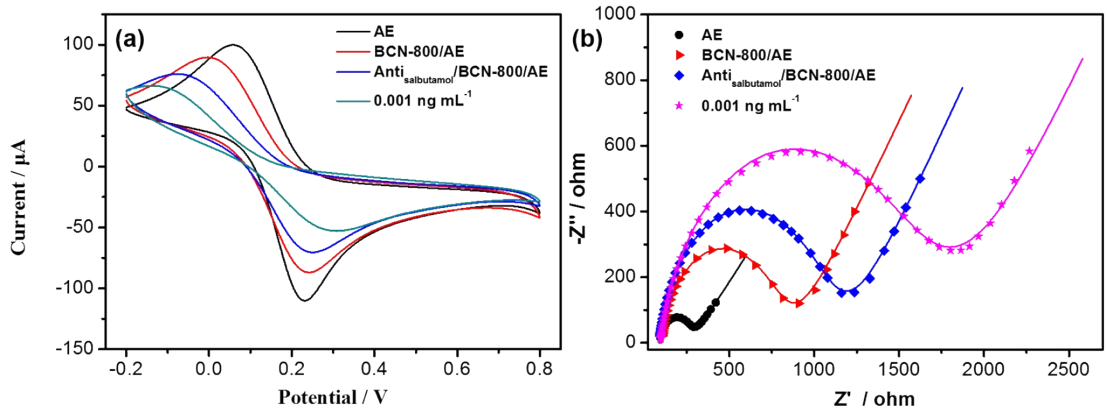


**Figure S15.** (a) CV at a scan rate of 100 mV $s^{-1}$ (b) EIS plots tracing the whole procedure of vomitoxin detection using the developed biosensor based on BCN-800, in 5 mM $[Fe(CN)_6]^{3-/4-}$ containing 0.14 M NaCl and 0.1 M KCl: AE, BCN-800/AE, $Anti_{salbutamol}$/BCN-800/AE, 0.001 ng $mL^{-1}$ salbutamol.

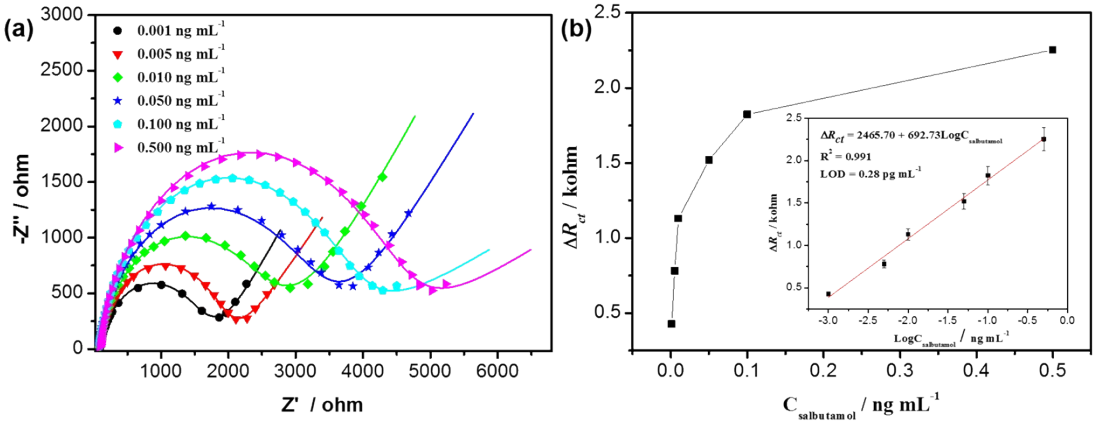


**Figure S16.** (a) EIS responses of the $Anti_{salbutamol}$/BCN-800/AE with different concentrations of vomitoxinn (0.001, 0.005, 0.01, 0.05, 0.1, and 0.5 ng $mL^{-1}$); (b) Dependence of $\Delta R_{ct}$ of the modified electrode on concentration of salbutamol. The linear part of the calibration curve is shown in the inset of (b).

To demonstrate the applicability of the developed biosensors in real-sample analysis, wine was analyzed using the BCN-800-based biosensor. As such, 1 mL of wine was diluted to 100 mL with PBS solution for the detection experiment. Different concentrations of vomitoxin were incorporated into the wine sample to test the recovery.Wine sample were purchased from a supermarket. The wine was from CASTEL *Depuis 1949*. The biosensor-based BCN-800 was directly immersed in wine samples, and 1.0 pg $mL^{-1}$ vomitoxin standard solution were added. The EIS spectra were recorded by CHI760E.

**Table S1** Determination of vomitoxin in wine by the immunosensor.

| Added (pg $mL^{-1}$) | Found (pg $mL^{-1}$) | Apparent recovery (%) |
|---|---|---|
| 1.0 | 0.97 | 97.0 |
| 5.0 | 4.98 | 99.6 |
| 10.0 | 10.01 | 100.1 |
| 50.0 | 50.15 | 100.3 |
| 100.0 | 99.85 | 99.9 |

**Table S2.** Comparisons of the proposed method with other vomitoxin-detection methods.

| Materials | Detection method | Line range | LOD | Ref |
|---|---|---|---|---|
| deoxynivalenol-3-glucoside | liquid chromatography/linear ion trap mass spectrometry | 10.0-200.0 μg $kg^{-1}$ | 30.0 μg $kg^{-1}$ | 4 |
| anti-deoxynivalenol | differential pulse voltammetry (DPV) | 0.01-1000.0 ng $mL^{-1}$ | 5.0 pg $mL^{-1}$ | 5 |
| Quenchbody | liquid chromatography and Mass spectrometry | 0.0003-3.0 mg $mL^{-1}$ | 0.006 mg $mL^{-1}$ | 6 |
| 516-MOFs/$Anti_{vomitoxin}$ | EIS | 0.001-0.5 ng $mL^{-1}$ | 0.7 pg $mL^{-1}$ | 7 |
| tris(bipyridine) ruthenium (II) chloride | EIS | 6.0-30.0 ng $mL^{-1}$ | 0.3 μg $mL^{-1}$ | 8 |
| BCN-900/ $Anti_{vomitoxin}$ | EIS | 0.001-0.5 ng $mL^{-1}$ | 0.32 pg $mL^{-1}$ | **This work** |

**Table S3** The atomic% of the BCN-based materials.

| Sample | Atomic% | | | |
|---|---|---|---|---|
| | N 1s | O 1s | C 1s | B 1s |
| BCN-700 | 2.17 | 47.91 | 12.74 | 37.18 |
| BCN-800 | 5.47 | 38.49 | 26.41 | 29.63 |
| BCN-900 | 6.85 | 33.57 | 30.98 | 28.60 |

**References**


1 W. Wang, L. Wang, L. Zou, G. Li, B. Ye, *J. Electroanal. Chem.* 2016, **772**, 17.
2 Q. Li, S. S. Zheng, X. Hu, Z. F. Shao, M. B. Zheng, H. Pang, ChemElectroChem 2018, **5**, 3859.
3 Q. Li, Z. F. Shao, T. Han, M. B. Zheng, H. Pang, *ACS Sustain. Chem. Eng*. 2019. DOI:10.1021/acssuschemeng.9b01148
4 M. Suman, E. Bergamini, D. Catellani, A. Manzitti, *Food Chem.* 2013, **136**, 1568.
5 Y. Qing, C. Li, X. Yang, X. Zhou, J. Xue, M. Luo, X. Xu, S. Chen, J. Qiu, *J. Appl. Electrochem.* 2016, **46**, 1049.
6 T. Yoshinari, H. Ohashi, R. Abe, R. Kaigome, H. Ohkawa, Y. Sugitakonishi, *Anal. Chim. Acta* 2015, **888**, 126.
7 C. S. Liu, C. X. Sun, J. Y. Tian, Z. W. Wang, H. F. Ji, Y. P. Song, S. Zhang, Z. H. Zhang, L. H. He, M. Du, *Biosens. Bioelectron.* 2017, **91**, 804.
8 C. Sunday, M. Masikini, L. Wilson, C. Rassie, T. Waryo, P. Baker, E. I. Iwuoha, *Sensors* 2015, **15**, 3854.